

## Theoretical Studies of 4,5-Diphenyl Imidazole Derivatives as Corrosion Inhibitors for Iron Protection by Density Functional Theory (DFT)

Muhamad Jalil Baari<sup>1\*</sup>, Alfiah Alif<sup>2</sup>, Muhammad Akbar S<sup>2</sup>, Kurniawan<sup>3</sup>, Fina Risnawati<sup>4</sup>

<sup>1</sup>Chemistry Department, Faculty of Science and Technology, Universitas Sembilanbelas November Kolaka, Jalan Pemuda, Kolaka, 93511, Indonesia

<sup>2</sup>Undergraduate Student of Chemistry Department, Faculty of Science and Technology, Universitas Sembilanbelas November Kolaka, Jalan Pemuda, Kolaka, 93511, Indonesia

\*Corresponding Author: [jalilbaari@gmail.com](mailto:jalilbaari@gmail.com)

Received: December, 12, 2023/Accepted: June, 10, 2024  
doi: 10.24252/al-kimiav12i1.43475

**Abstract:** Corrosion is a serious problem in the petroleum industry. The use of corrosion inhibitors is an effort to reduce the corrosion rate on metal materials. This study used the computational chemistry approach to investigate the corrosion inhibition performances of 4,5-diphenyl imidazole and its derivatives with additional substituents, for instance, electron acceptors and electron donors. Geometry optimizations and calculations of molecular frontier orbital energies were conducted using density functional theory (DFT) in the aqueous phase. These frontier orbital energy values were used to determine other reactivity and stability parameters, such as band gap energy, electron affinity, ionization potential, chemical hardness, chemical softness, number of electron transfers, chemical potential, nucleophilicity, electrophilicity, electronegativity, back donation energy, and interaction energy. Electrostatic potential, Mulliken atomic charge, and theoretical inhibition efficiency of 4,5-diphenyl imidazole derivatives were also determined. Generally, the presence of electron donor substituents theoretically increases corrosion inhibitors. The 4,5-diphenyl imidazole with  $-NH_2$  substituent is a better derivative than others based on several reactivity and stability parameters due to adding adsorption centers. Therefore, it can increase the performance of 4,5-diphenyl imidazole as a corrosion inhibitor. The adsorption behaviors of 4,5-diphenyl imidazole and its derivatives on Fe(100) surfaces were investigated using molecular dynamics simulation. The binding energies of three types of inhibitors on the Fe surface of studied inhibitors followed the order:  $D-NH_2 > 4,5\text{-diphenyl imidazole (D)} > D-NO_2$ . This ranking obtained is consistent with the theoretical inhibition efficiency.

**Keywords:** 4,5-diphenyl imidazole derivatives, Corrosion inhibitor, DFT method, Iron

### INTRODUCTION

Corrosion generally relates to the degradation of a material's quality. Corrosion, specifically for metal, involves electrochemical reactions that release metal ions and electrons on the metal surface (Revie & Uhlig, 2008). These reactions occur faster in a humid or watery environment. In addition, acid solution and mineral salts in a fluid system inflict severe corrosion. Corrosion is undoubtedly detrimental to various sectors, especially the petroleum industry because its principal equipment is fabricated from metal. The most affected device is the pipeline, which carries fluids containing oil, gas, mineral salts, and

microorganisms from oil sources to the preparation and production facilities (Qiang et al., 2017; Xiang et al., 2017).

Consequently, repair costs are needed, and cessation of production cannot be avoided. Besides that, it will also threaten employee safety and environmental preservation (Chaussemier et al., 2015). Corrosion inhibitor utilization is still famous for controlling corrosion in fluid systems. It corresponds to the effective, practical, and economical way for the inner part of the pipeline protection. The inhibition mechanism occurs through adsorption, which is continued by forming a protective layer amid metal and fluids (Lv et al., 2019).

Several experimental studies concerning metal protection with corrosion inhibitors have been conducted. Most organic compounds were recommended due to environmental sustainability factors (Baari et al., 2021; Martinović et al., 2021; Subekti et al., 2020). Imidazole derivatives are widely used organic compounds as corrosion inhibitors (Ismail et al., 2019; Marušić et al., 2018; Srivastava et al., 2017; Zunita et al., 2020). These compounds have high corrosion inhibition efficiency after being experimentally tested by weight-loss and electrochemical methods. Their performances are affected by heteroatoms with lone pair electrons and  $\pi$  electrons/double bonds (Ashassi-Sorkhabi et al., 2005; Baari & Sabandar, 2021). The first example is benzimidazole derivatives in 1 M  $\text{H}_3\text{PO}_4$  solution. The reduction of corrosion rate on the carbon steel after attaching electron donor substituent ( $-\text{NH}_2$ ) to benzimidazole was quite significant compared to unsubstituted benzimidazole (Ghanbari et al., 2010). Then, adding electron acceptor ( $-\text{Cl}$ ) and electron donor ( $-\text{CH}_3$ ) substituents in the tetraphenyl imidazole compound could reduce mild steel corrosion in 0.5 M  $\text{H}_2\text{SO}_4$ . Inhibition efficiencies reach 96% for  $-\text{Cl}$  and 92% for  $-\text{CH}_3$ , respectively (Ouakki et al., 2019). Elyoussfi et al., 2023 analyzed two imidazopyridine derivatives as corrosion inhibitors for mild steel protection in 1 M HCl solution. Imidazopyridine derivatives containing  $-\text{OH}$  substituent could improve corrosion inhibition efficiency by up to 92%, whereas another one with  $-\text{NO}_2$  substituent only has an inhibition efficiency of 86% (Elyoussfi et al., 2023).

However, only a few computational studies were conducted to compare or make molecular models. Computational chemistry research can determine quantum parameters based on physicochemical properties and electronic structures through theoretical calculations (Baari, 2023; Tsuneda, 2014). It can support experimental results for better information and find novel potential compounds as corrosion inhibitors. Hence, this subject is of great interest. A method that accurately calculates and models multiple electron systems like imidazole derivatives is density functional theory (DFT). This method can optimize and determine the electronic structure of atoms and molecules (Mustafa & Mamand, 2019). A previous study indicates that the DFT method has been used to observe the substituents or functional groups on the performance of imidazole derivatives as corrosion inhibitors for iron metal (Leng et al., 2023).

Meanwhile, Wahyuningrum had synthesized 4,5-diphenyl imidazole as a corrosion inhibitor (Wahyuningrum, 2008). However, theoretical studies concerning its corrosion inhibition have yet to be informed. This study aims to analyze the performances of several 4,5-diphenyl imidazole derivatives as corrosion inhibitors based on structural and quantum parameters. Optimized structures are obtained by the DFT method to observe the effects of additional functional substituents consisting of electron acceptors and electron donors. The impact of the different substituents on the less reactive site (carbon number 2 on the

imidazole ring) will change the reactivity as a whole of 4,5-diphenyl-imidazole derivatives. Besides that, the reactivity of nitrogens on the imidazole ring will also be investigated.

The analysis does not only observe the effect of substituents like  $-\text{OH}$ ,  $-\text{CH}_3$ ,  $-\text{Cl}$ , and  $-\text{NO}_2$ , but also other potential substituents like  $\text{CHO}$ ,  $\text{COOH}$ , and  $\text{F}$ , as electron acceptors, and  $\text{CH}_2\text{OH}$ ,  $\text{CH}_3$ ,  $\text{CH}_2\text{CH}_3$  as electron donors. Therefore, novel potential inhibitors can be obtained and synthesized in future research.

## RESEARCH METHODS

### Materials and Instruments

The molecular objects used in this study were 4,5-diphenyl imidazole (Figure 1) and its derivatives, water ( $\text{H}_2\text{O}$ ), and iron atom ( $\text{Fe}$ ). The laptop's specifications were an AMD Ryzen 7 (6800 series) processor with 3.2 GHz, 24 GB of RAM, and 512 GB of SSD. Quantum chemistry calculations were done using Orca software version 5.0.3 (Neese, 2022). Other software used in this study were Avogadro, Notepad++, IboView, Chemcraft, and Gabedit.

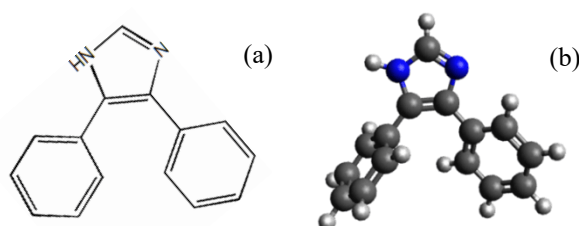


Figure 1 Molecular structure of 4,5-diphenyl imidazole (a) 2D (b) 3D

Several 4,5-diphenyl imidazole derivatives that consist of electron-withdrawing and releasing substituents in this study are shown in Figure 2. Furthermore, input files were obtained from Avogadro software based on atom coordinates in molecular structures. Gabedit software adjusted the applied method and basis set.

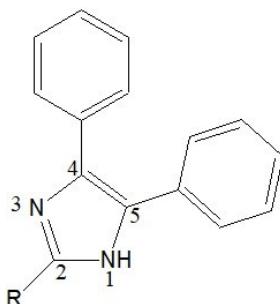


Figure 2 Molecular structure of 4,5-diphenyl imidazole with additional substituents.  $\text{R} = -\text{CHO}$ ,  $-\text{COOH}$ ,  $-\text{NO}_2$ ,  $-\text{F}$ ,  $-\text{Cl}$  (as electron acceptors) and  $\text{R} = -\text{OH}$ ,  $-\text{CH}_2\text{OH}$ ,  $-\text{NH}_2$ ,  $-\text{CH}_3$ ,  $-\text{CH}_2\text{CH}_3$  (as electron donors).

### Quantum Parameters Calculations

Geometry optimization and electronic parameters consisting of lowest unoccupied molecular orbital ( $E_{LUMO}$ ) and highest occupied molecular orbital energies ( $E_{HOMO}$ ) were calculated by Orca software version 5.0.3 through Gabedit (Allouche, 2011; Neese, 2022). This study applied hybrid functionals, including the three-parameter Becke potential and the Lee-Yang-Parr hybrid correlation functions (B3LYP). These functions combined the advantages of Hartree-Fock theory (HF) and local density approximation (LDA) for a more accurate description of the electronic molecular structure. 6-31G is the basis set, and d,p functions within that basis set are polarization functions added to all atoms. It allows charge polarization away from the atomic distribution. This study was conducted in the aqueous phase (water as a solvent), using the Conductor-like Polarizable Continuum Model or CPCM.

The band gap energy ( $\Delta E$ ), electron affinity ( $A$ ), and ionization potential ( $I$ ) were determined based on Koopman's theorem. The Mulliken atomic charge was also obtained from these calculations. Obtained values of  $A$  and  $I$  contributed to determine other reactivity and stability parameters that affect corrosion inhibition efficiency, such as chemical hardness ( $\eta$ ), chemical softness ( $\sigma$ ), number of electron transfers ( $\Delta N$ ), chemical potential ( $\mu$ ), nucleophilicity ( $\epsilon$ ), electrophilicity ( $\omega$ ), electronegativity ( $\chi$ ), back donation energy ( $\Delta E_{BD}$ ), and energy interaction ( $\Delta E_{Int}$ ). The following equations calculated various quantum parameters:

$$I = -E_{HOMO} \quad [1]$$

$$A = -E_{LUMO} \quad [2]$$

$$\Delta E = E_{LUMO} - E_{HOMO} \quad [3]$$

$$\chi = \frac{-E_{HOMO} - E_{LUMO}}{2} \quad [4]$$

$$\eta = \frac{E_{LUMO} - E_{HOMO}}{2} \quad [5]$$

$$\sigma = \frac{1}{\eta} \quad [6]$$

$$\mu = -\chi \quad [7]$$

$$\omega = \frac{\mu^2}{2\eta} \quad [8]$$

$$\epsilon = \frac{1}{\omega} \quad [9]$$

$$\Delta N = \frac{\chi_{Fe} - \chi_{inh}}{2(\eta_{Fe} + \eta_{inh})} \quad [10]$$

$$\Delta E_{BD} = -\frac{\eta}{4} \quad [11]$$

$$\Delta E_{Int} = -\frac{(\chi_{Fe} - \chi_{inh})^2}{4(\eta_{Fe} + \eta_{inh})} \quad [12]$$

$\chi_{Fe}$  and  $\chi_{inh}$  are the electronegativities of the iron and inhibitor, respectively. Meanwhile,  $\eta_{Fe}$  and  $\eta_{inh}$  are the hardnesses of the iron and inhibitor. Exclusively for the iron, theoretical value  $\chi_{Fe}$  is 7 eV and  $\eta_{Fe}$  is 0 eV since bulk iron is chemically softest (Al-Qurashi & Wazzan, 2022; Quy Huong et al., 2019).

### Output Data Visualization

Notepad++ was used to observe output data. Then, Iboview software visualized the optimized geometry structure, HOMO contour, and LUMO contour of 4,5-diphenylimidazole and its derivatives (Knizia, 2013). Furthermore, the electrostatic potential and Mulliken atomic charges were visualized by Avogadro and Chemcraft software, respectively (Hanwell et al., 2012; Zhurko and Zhurko, 2015).

### Molecular Dynamics Simulation

The adsorption behaviour of 4,5-diphenylimidazole and its derivatives on the Fe(100) surface was studied by molecular dynamics simulation using the forcite module in Material Studio 2020 software. The Fe(100) surface was chosen due to its most straightforward low relative index surface of iron, and it has been used for specimen substrate in the investigation of adsorption models (Chen et al., 2020). A vacuum slab on the top side with a thickness of 20 Å was built using Crystal Builder. The force field in this simulation applied condensed-phase-optimized molecular potentials for atomistic simulation studies (COMPASS). The canonical ensemble NVT was performed at 298 K, and the Andersen thermostat was used to control the temperature (Andersen, 1980). Simulation time was set to 1000 ps with a time step of 1.0 fs.

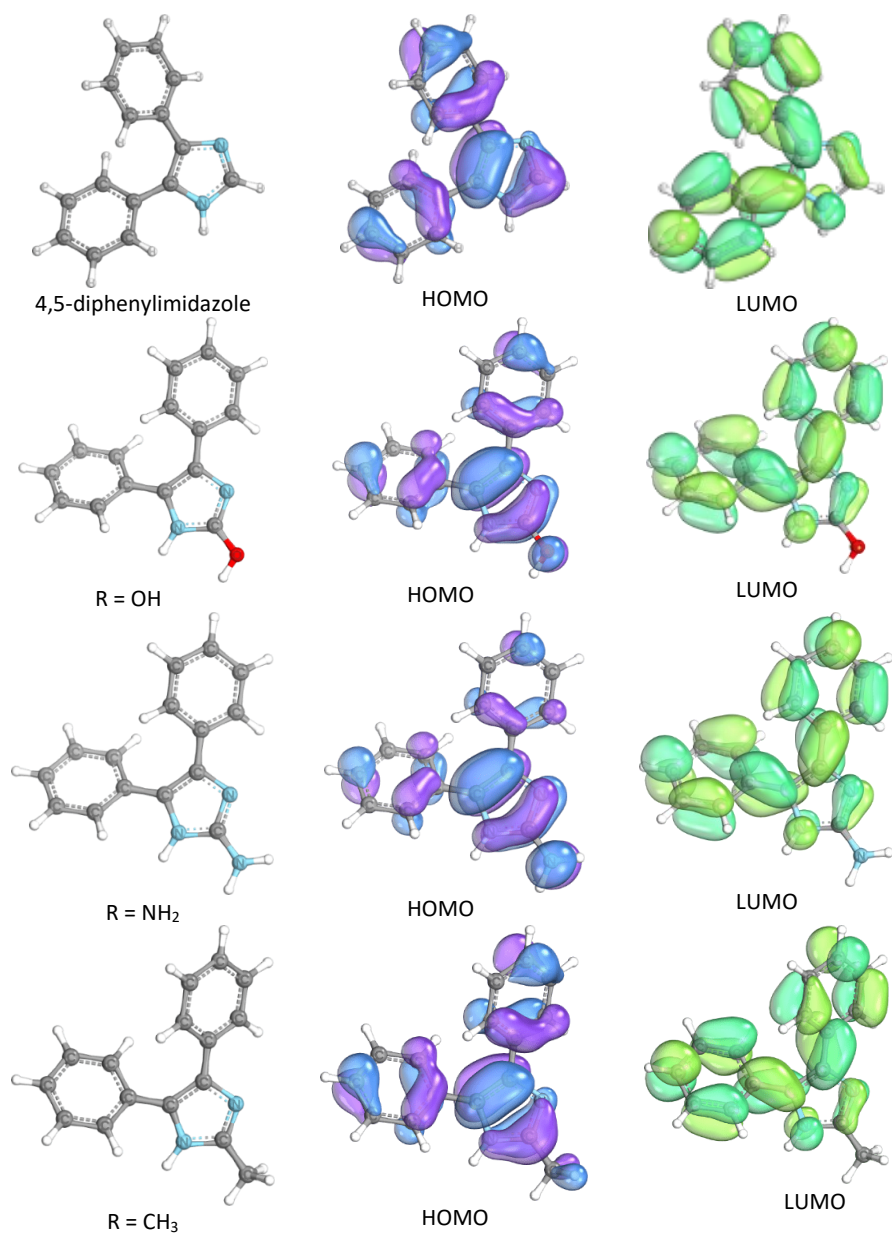
## RESULTS AND DISCUSSION

### Structure and Active Site of Corrosion Inhibitor

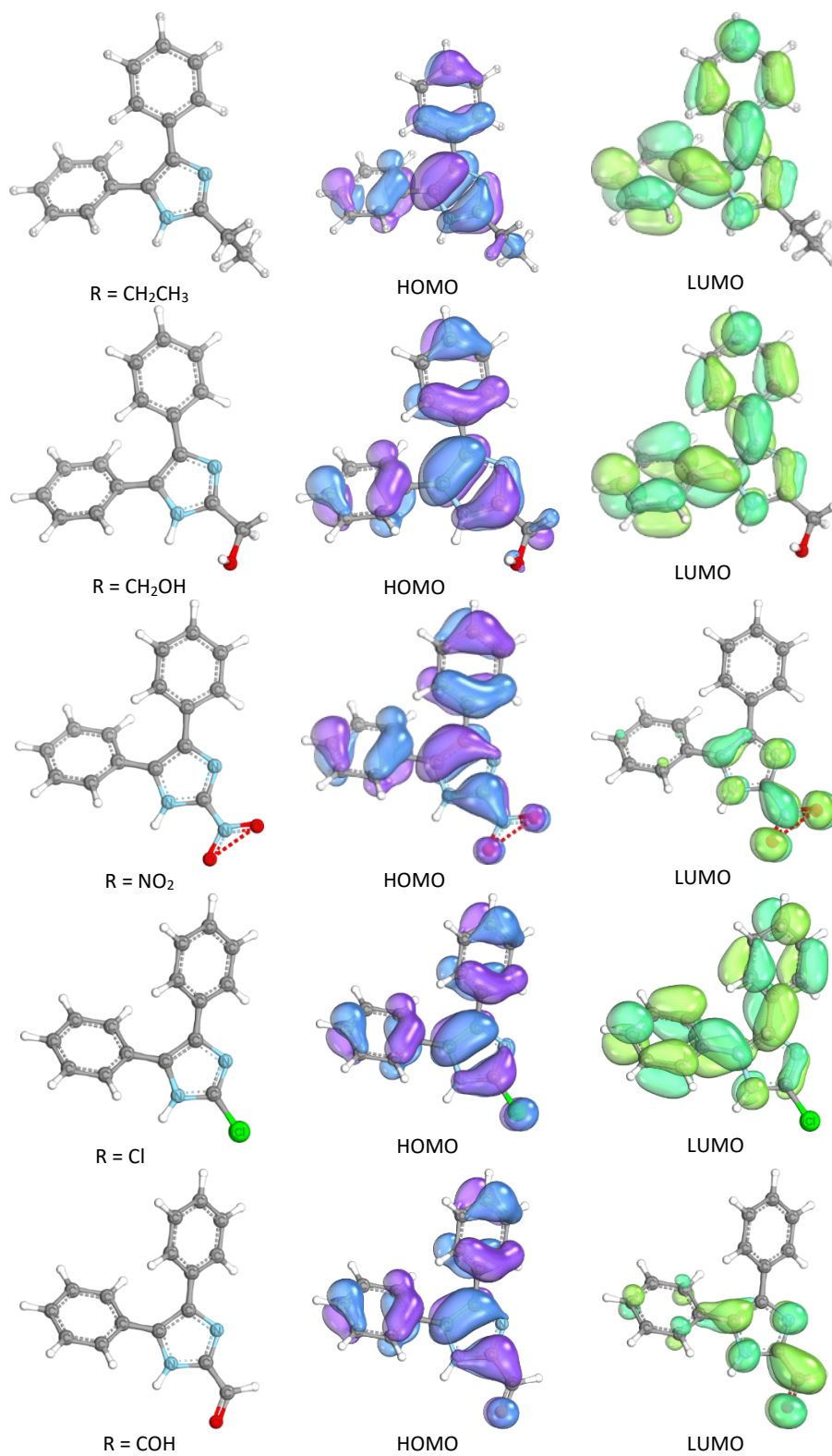
The molecular structures of 4,5-diphenyl imidazole and its derivatives with additional substituents as electron acceptors and donors were manufactured by Avogadro (Hanwell et al., 2012). Several substituents were chosen based on previous research observations and the convenience synthesis of 4,5-diphenyl imidazole derivatives with available organic reactants. The basis set used the Pople style with modifications or split valence basis set (6-31G). A split valence basis set will only increase the size of the orbitals, but it cannot overcome changes in the shape of the orbitals. Hence, functions (d,p) were used to apply the polarization functions on all atoms in 4,5-diphenylimidazole derivatives (Neese et al., 2022). To describe each atom, these polarisation functions increase angular momentum beyond the ground state.

The results obtained from calculations are the optimized molecular geometry and quantum parameters that specify the performance and mechanism of 4,5-diphenyl imidazole derivatives against iron corrosion, such as HOMO-LUMO contours and HOMO-LUMO energies. Figures 3 and 4 depict optimized geometric structures, as well as HOMO and LUMO contours of 4,5-diphenyl imidazole and its derivatives within a water environment. Understanding these molecules' behaviour in the aqueous environment is crucial for corrosion inhibitor applications. The appearance of water can significantly influence the electronic properties and stability of these compounds. Hence, visualizing their molecular structures in such conditions is essential for predicting their behaviour accurately. The images of HOMO and LUMO contours describe the interaction areas among inhibitor molecules and iron atoms/ions. HOMO contours indicate the sites with a

propensity to donate electrons (Oyenehin et al., 2022). On the contrary, the sites preferred as electron acceptors are shown in LUMO contours (Wang et al., 2020).







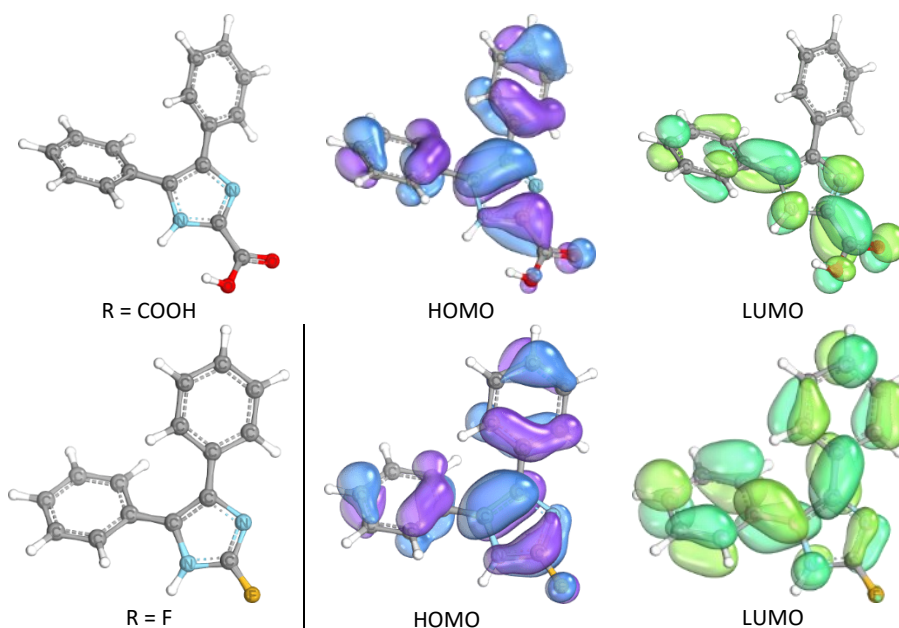


**Figure 4.** Optimized geometry, HOMO, and LUMO of 4,5-diphenylimidazole derivatives with electron acceptor and donor substituents obtained by B3LYP/6-31G(d,p) CPCM(water)

HOMO contours also describe that most electrons transfer from inhibitor to metal occurs in phenyl and imidazole rings. The presence of electron donor substituents like  $-\text{NH}_2$ ,  $-\text{CH}_3$ ,  $-\text{OH}$ , and  $-\text{CH}_2\text{OH}$  serves as additional centres of electron transfer to metal. However, these substituents complicate the withdrawal of electrons from the back-donation process on the anode side and the iron cathode. The absence of any LUMO contour around the substituents supports it. Meanwhile, the 4,5-diphenyl imidazole derivatives with additional  $-\text{NO}_2$ ,  $-\text{COH}$ , and  $-\text{COOH}$  revoke the phenyl groups' ability to attract electrons in cathode sites. It is displayed on phenyl groups that do not have LUMO contours. Consequently, the electron transfer phenomenon in these derivatives will decrease.

Electrostatic potential relates to the effect of molecular net electrostatic in specified sites based on electron density distribution (Bendjeddou et al., 2016). These cover maps denote the region most and least electrons occupy at inhibitor molecules. The red covers signify areas with higher electron density, whereas the blue covers indicate the opposite. A white surface marks moderate electron density. Therefore, nitrogen atoms with red covers in the imidazole rings act as electron donors.

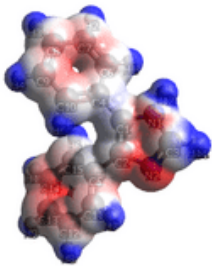
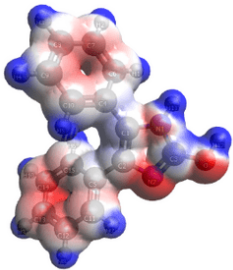
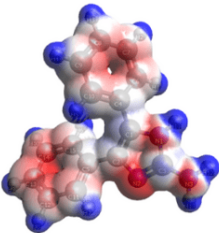
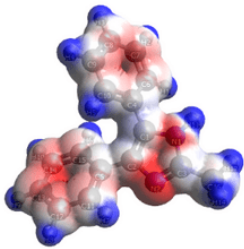
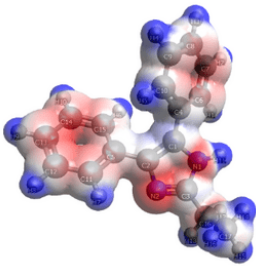
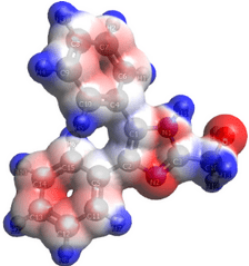
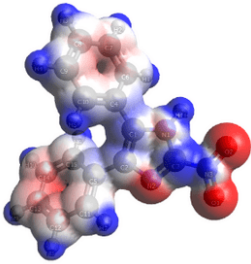
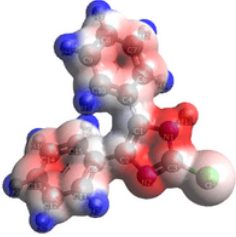
Table 1 shows the electrostatic potential of 4,5-diphenylimidazole derivatives with electron acceptor and electron donor substituents. The electron density or active sites of derivatives with electron donor substituents are more located in  $-\text{OH}$ ,  $-\text{CH}_2\text{OH}$ , or  $-\text{NH}_2$ . Nevertheless, in the 4,5-diphenyl imidazole with  $-\text{CH}_3$  substituent, the active site tends to be located in the imidazole ring. Electrostatic potential cover maps of 4,5-diphenyl imidazole with electron acceptor substituents display electron density around oxygen for  $-\text{COH}$  and  $-\text{COOH}$  substituents. However, since these substituents attract electrons on the iron cathode sites, interactions with the iron on the anode sites are usually less favourable. The partial positive charge on the element directly inserted into the ring generates a

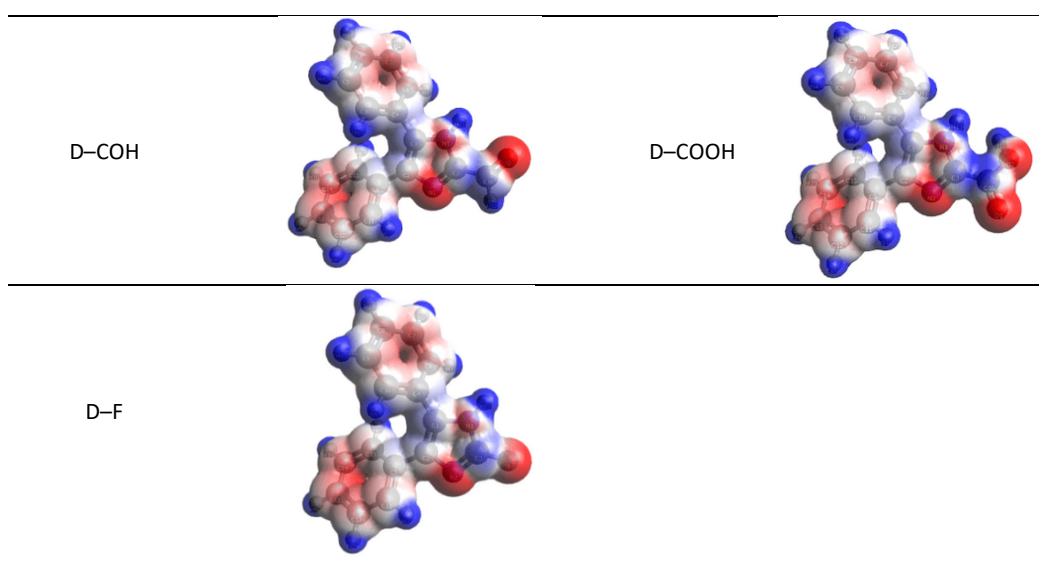


moderate electron-withdrawing inductive effect. Hence, additional  $-\text{COH}$  and  $-\text{COOH}$  substituents make the aromatic rings relatively poor electrons.

Table 1 also shows the higher electron density on heteroatoms, except for the Cl substituent. It is affected by the inductive effect of electrons on the electronegative atoms. Consequently, electronegative atoms have higher electron density, or the red colour is sharper, whereas electropositive atoms have lower electron density, or the blue colour is sharper. However, the electron density of  $-\text{Cl}$  and  $-\text{CH}_3$  substituents relatively decreases because the induction effect leads to the nitrogen in the imidazole ring.

**Table 1.** Electrostatic potential of 4,5-diphenylimidazole derivatives by B3LYP/6-31G(d,p) by the presence of electron-acceptor and donor substituents

Inhibitor	Electrostatic potential map	
4,5-diphenylimidazole (D)		D-OH 
D-NH <sub>2</sub>		D-CH <sub>3</sub> 
D-CH <sub>2</sub> CH <sub>3</sub>		D-CH <sub>2</sub> OH 
D-NO <sub>2</sub>		D-Cl 



The electrostatic potential map relates to the corrosion inhibition mechanism. It is initiated by the adsorption of inhibitor molecules on the metal surface (Lv et al., 2019). Imidazole rings and additional substituents with heteroatoms (N and O) become active sites at the center of adsorption. Inhibitor adsorption can happen through physical adsorption, chemical adsorption, and both. Adsorption energy in the form of standard Gibbs free energy of the adsorption ( $\Delta G^{\circ}_{ads}$ ) determines the adsorption type. Van der Waals interactions assign physical adsorption, whereas chemical adsorption involves electron sharing.

#### Quantum Chemical Parameter of Corrosion Inhibitor and Theoretical Inhibition Efficiency

Quantum chemical parameters corresponding to the performance of 4,5-diphenylimidazole derivatives as corrosion inhibitors were theoretically determined. These parameters consist of LUMO energy, HOMO energy, band gap energy, electron affinity, ionization potential, chemical hardness, chemical softness, chemical potential, nucleophilicity, electrophilicity, electronegativity, number of electron transfers, back donation energy, and interaction energy. All parameters provide information regarding the stability and reactivity of a corrosion inhibitor (Obot et al., 2016). Calculation results are listed in Tables 2 and 3. 4,5-diphenylimidazole derivatives with electron donor substituents perform better based on quantum parameters values than unsubstituted 4,5-diphenylimidazole. A molecule with higher HOMO energy (more positive) readily donates its electrons to the lowest unoccupied molecular orbital (LUMO) of Fe (Kaya et al., 2016). The value of HOMO energy follows the order of: D-NH<sub>2</sub> > D-OH > D-CH<sub>3</sub> > D-CH<sub>2</sub>CH<sub>3</sub> > D-CH<sub>2</sub>OH > D > D-F > D-Cl > D-COOH > D-COH > D-NO<sub>2</sub>. Conversely, the electron acceptor ability will be influenced by LUMO energy. A higher value of LUMO energy (less negative) complicates inhibitor molecules for drawing electrons (Madkour & Elshamy, 2016). It represents a mixed-type inhibitor, predominantly an anodic-type inhibitor. The value of LUMO energy follows the order of D-NH<sub>2</sub> > D-CH<sub>3</sub> > D-CH<sub>2</sub>CH<sub>3</sub> > D > D-CH<sub>2</sub>OH > D-OH > D-F > D-Cl > D-COOH > D-COH > D-NO<sub>2</sub>.

Nucleophilicity ( $\epsilon$ ) relates to the reactivity of electron-rich molecules toward Fe ions as electron-deficient species. Derivatives with larger nucleophilicity prefer to release

electrons than accept electrons. The nucleophilicity sequence is  $D-NH_2 > D-CH_3 > D-CH_2CH_3 > D-OH > D-CH_2OH > D > D-F > D-Cl > D-COOH > D-COH > D-NO_2$ . Electrophilicity ( $\omega$ ) is the inverse of nucleophilicity. This parameter expresses the electrophilic power of a compound.  $\omega$  is associated with chemical hardness and electronegativity. The electrophilicity sequence is  $D-NH_2 < D-CH_3 < D-CH_2CH_3 < D-OH < D-CH_2OH < D < D-F < D-Cl < D-COOH < D-COH < D-NO_2$ . A good inhibitor has larger nucleophilicity and lower electrophilicity. Augmentation of the  $NH_2$  substituent in 4,5-diphenylimidazole generates better nucleophilicity and electrophilicity in the aqueous phase. Hence, interaction with the Fe atom/ion will be favorable. In this case, water molecules contribute to stabilizing lone pair electrons in the molecular orbitals (Neese et al., 2022).

Electron affinity ( $A$ ) and ionization potential ( $I$ ) are stability parameters obtained from negative values of  $E_{LUMO}$  and  $E_{HOMO}$ , respectively. Reactive anodic inhibitors have a relatively small ionization potential to release electrons easily. Otherwise, electron affinity ( $A$ ) corresponds to the facility of 4,5-diphenylimidazole derivatives to attract electrons from the back donation process. 4,5-diphenylimidazole derivatives with slight ionization potential and electron affinity, like  $D-NH_2$ , are chemically stable and do not prefer attracting electrons from the back donation process (Wazzan, 2015). However, they can be nice anodic inhibitors or mixed-type inhibitors. Meanwhile,  $D-NO_2$  and  $D-COH$  have the largest electronic affinity. Hence, this derivative behaves as a cathodic-type inhibitor through electron withdrawing on the cathode site. Besides that, the electron-back donation is preferable if its electrons are shared with the metal/metal ion on the anode site.

Band gap energy ( $\Delta E$ ) is an important chemical quantum parameter for inhibitor molecules' adsorption and binding stability on the Fe surface (Obot et al., 2016; Wazzan, 2015). It is calculated through the difference between LUMO and HOMO energies. Small band gap energy signifies the convenience of corrosion inhibitors to release electrons because the required energy to move electrons from HOMO is relatively low (Madkour & Elshamy, 2016). The value of  $\Delta E$  follows the order of:  $D-NO_2 < D-COH < D-NH_2 < D-OH < D-COOH < D-CH_3 < D-CH_2CH_3 < D-CH_2OH < D-F < D-Cl < D$ .

**Table 2.** Calculation results of quantum chemical parameters for 4,5-diphenylimidazole derivatives by the presence of electron-acceptor and donor substituents in the aqueous phase

Inhibitor	E HOMO /eV	E LUMO /eV	I/eV	A/eV	$\Delta E$ /eV	$\chi$ /eV	$\eta$ /eV	$\sigma$ /eV <sup>-1</sup>	$\omega$ /eV	$\epsilon$ /eV <sup>-1</sup>
D	-5.426	-0.754	5.426	0.754	4.672	3.090	2.336	0.428	2.044	0.489
D-NO <sub>2</sub>	-5.935	<b>-2.601</b>	5.935	<b>2.601</b>	<b>3.334</b>	4.268	<b>1.667</b>	<b>0.600</b>	5.464	0.183
D-Cl	-5.518	-0.871	5.518	0.871	4.646	3.195	2.323	0.430	2.196	0.455
D-COH	-5.729	-1.758	5.729	1.758	3.971	3.744	1.985	0.504	3.529	0.283
D-COOH	-5.722	-1.326	5.722	1.326	4.397	3.524	2.198	0.455	2.824	0.354
D-F	-5.443	-0.856	5.443	0.856	4.587	3.150	2.294	0.436	2.162	0.462
D-NH <sub>2</sub>	<b>-4.711</b>	<b>-0.716</b>	<b>4.711</b>	<b>0.716</b>	3.995	<b>2.713</b>	1.998	0.501	<b>1.842</b>	<b>0.543</b>
D-CH <sub>2</sub> OH	-5.337	-0.764	5.337	0.764	4.574	3.050	2.287	0.437	2.034	0.492
D-OH	-5.135	-0.777	5.135	0.777	4.358	2.956	2.179	0.459	2.005	0.499
D-CH <sub>3</sub>	-5.280	-0.731	5.280	0.731	4.549	3.006	2.275	0.440	1.986	0.504
D-CH <sub>2</sub> CH <sub>3</sub>	-5.291	-0.739	5.291	0.739	4.552	3.015	2.276	0.439	1.997	0.501

**Table 3.** Calculation results of electron transfers, back donation energy, and interaction energy parameters for 4,5-diphenylimidazole derivatives by the presence of electron-acceptor and donor substituents in the aqueous phase

Inhibitor	$\mu$ /eV	$\Delta N$	$\Delta E_{BD}$ /eV	$\Delta E_{Int}$ /eV
4,5-diphenyl imidazole (X)	-3.0898	0.8370	-0.5839	-1.6364
R-NO <sub>2</sub>	-4.2679	0.8195	<b>-0.4167</b>	-1.1195
R-Cl	-3.1946	0.8190	-0.5808	-1.5583
R-COH	-3.7435	0.8201	-0.4963	-1.3353
R-COOH	-3.5240	0.7906	-0.5496	-1.3740
R-F	-3.1496	0.8393	-0.5734	-1.6159
R-NH <sub>2</sub>	<b>-2.7132</b>	<b>1.0729</b>	-0.4994	<b>-2.2997</b>
R-CH <sub>2</sub> OH	-3.0502	0.8636	-0.5717	-1.7055
R-OH	-2.9560	0.9280	-0.5447	-1.8764
R-CH <sub>3</sub>	-3.0058	0.8780	-0.5687	-1.7534
R-CH <sub>2</sub> CH <sub>3</sub>	-3.0152	0.8754	-0.5690	-1.7440

Furthermore, chemical hardness and softness correspond to the ability of a molecule to withstand deformation and polarization of electron clouds (Kaya et al., 2016). These parameters provide information about molecular stability obtained from band gap energy. Molecules with significant chemical hardness tend to hold their electrons rather than release electrons (Kaya et al., 2016). Thus, its corrosion inhibition performance in the anode site will not be good enough. Chemical softness is inversely proportional to hardness, so 4,5-diphenylimidazole derivatives with more softness will be preferable to share electrons based on the simplicity of adsorption (Zarrouk et al., 2013). This condition is appropriate with the hard and soft acids and bases (HSAB) theory, in which a soft material like bulk iron prefers interacting with another soft material. The value of  $\eta$  follows the order of: D-NO<sub>2</sub> < D-COH < D-NH<sub>2</sub> < D-OH < D-COOH < D-CH<sub>3</sub> < D-CH<sub>2</sub>CH<sub>3</sub> < D-CH<sub>2</sub>OH < D-F < D-Cl < D. This order is inversely proportional to chemical softness ( $\sigma$ ). Therefore, 4,5-diphenylimidazole with NO<sub>2</sub> substituent is the best corrosion inhibitor based on chemical hardness and softness parameters in the aqueous phases.

The electronegativity of a molecule also affects the protection ability of an inhibitor. It corresponds to the propensity of atoms, ions, or molecules to pull electrons in the chemical bonds and to transfer electrons involving inhibitors and metals. In contrast, the chemical potential is a negative value of electronegativity. The electron transfer occurs from inhibitor molecules with lower electronegativity to iron surfaces with higher electronegativity until the equality of electronegativity and chemical potential is achieved (Madkour & Elshamy, 2016). Corrosion inhibitors should have smaller electronegativities because electrons in the chemical bond will be interested in the iron side. 4,5-diphenylimidazole with NH<sub>2</sub> substituent has a higher chemical potential (less negative) that facilitates interactions among Fe ions and inhibitor molecules.

The reactivity parameters of a corrosion inhibitor toward Fe are also represented by the number of electron transfers, back donation energy, and interaction energy. The difference in electronegativity drives the number of electron transfers ( $\Delta N$ ). Otherwise, chemical hardness hinders electron transfer (Rodríguez-Valdez et al., 2005). Highly soft

inhibitor molecules will facilitate electron transfer from the inhibitor to the iron (Wazzan & Mahgoub, 2014). The 4,5-diphenylimidazole with  $\text{NH}_2$  substituent shows higher  $\Delta N$  than other derivatives. Nevertheless, the values of the electron transfer for all derivatives are greater than zero ( $\Delta N > 0$ ) in the water environment. Therefore, all inhibitor molecules prefer to donate electrons, while Fe accepts electrons (Al-Qurashi & Wazzan, 2022).

Back-donation energy ( $\Delta E_{BD}$ ) correlates to the electron back-donation processes from Fe to inhibitor molecules after electron donation from the inhibitor to the unfilled d-orbital of the Fe.  $\Delta E_{BD}$  was calculated from the chemical hardness of the inhibitor molecule. Higher back-donation energy (less negative) indicates better corrosion inhibition performance, especially for cathodic-type inhibitors. Thus, 4,5-diphenylimidazole with  $\text{NO}_2$  substituent can attract electrons more strongly from the back-donation process than other substituents. The interaction energy between Fe-inhibitor molecules is a chemical parameter in an anti-corrosion system. Similar to the electron transfer parameter, it was obtained from the electronegativity and chemical hardness of Fe and inhibitor molecules, respectively. A good corrosion inhibitor has relatively high interaction energy (more negative) (Mi et al., 2015). Because of the linear relationship between interaction and binding energies, more negative interaction energy indicates high binding energy. As a result, Fe-inhibitor bonds become vigorous (Guo et al., 2017).

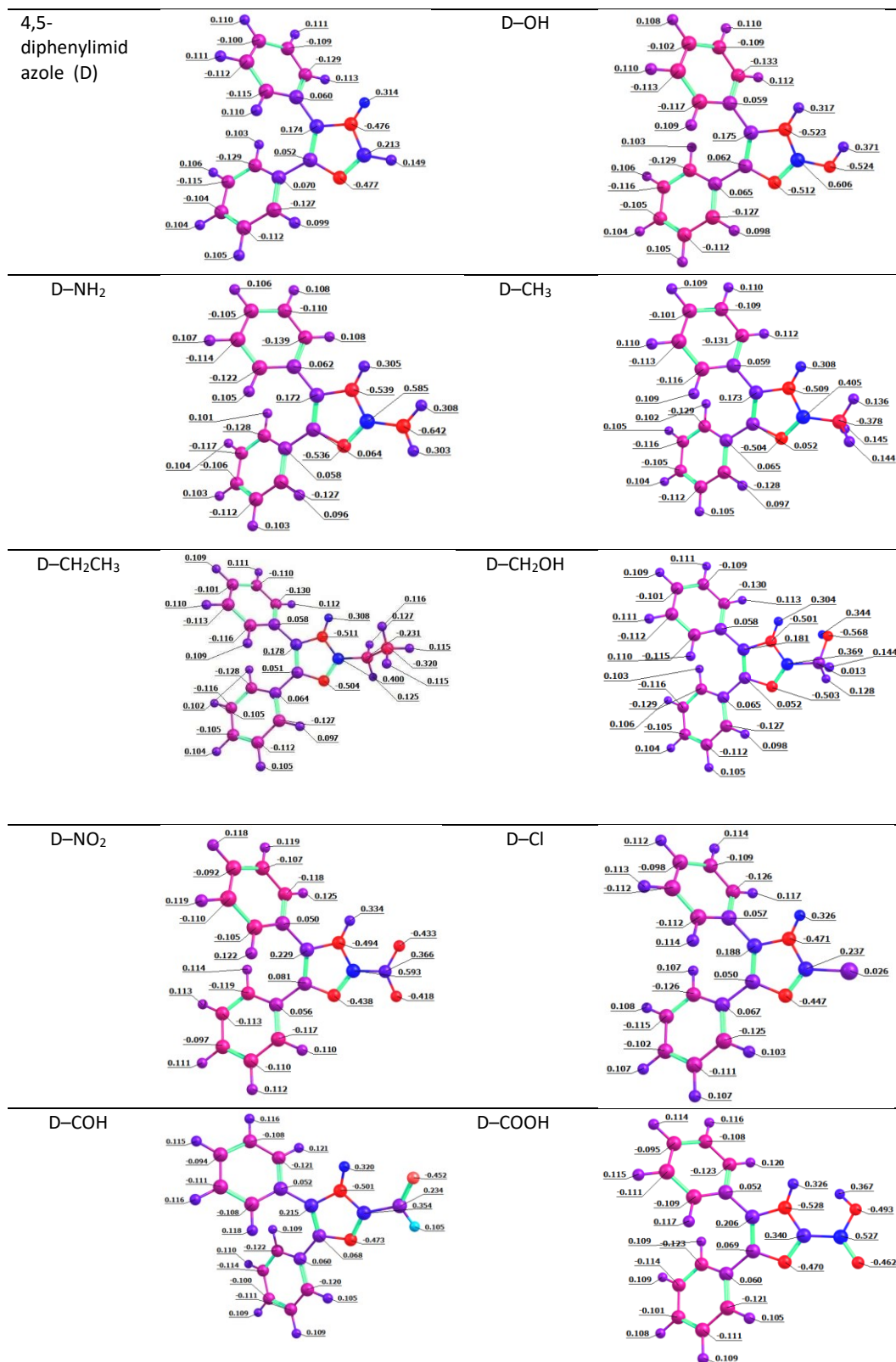
Mulliken charges provide information about asymmetric charge distribution and estimating partial atomic charges from calculations conducted by computational methods (Oyenyin et al., 2022). Partial atomic charges with more negative values usually readily donate electrons to the metal's unoccupied orbital (Madkour & Elroby, 2015). Hence, these atoms are inhibitor molecules' adsorption sites when contacting with metal atoms/metal ions. This parameter is usually in good agreement with potential electrostatic maps. Hydration by the presence of water molecules can raise the dipole moment and change the electronic structure slightly, reflecting stronger interactions among 4,5-diphenylimidazole derivatives with Fe (Guo et al., 2017).

Unsubstituted 4,5-diphenyl imidazole only has an adsorption site on imidazole rings through two nitrogen atoms. Extra nitrogen in the  $-\text{NH}_2$  group and the oxygen atom in  $-\text{OH}$  or  $-\text{CH}_2\text{OH}$  groups create additional adsorption sites in 4,5-diphenylimidazole derivatives based on Mulliken charges. In addition, two nitrogens in the imidazole ring can still possibly be interaction sites. Partial atomic charges of nitrogens on imidazole rings can vary depending on inserted substituent types. The most negative charges (red colour) of nitrogen imidazoles ring occur in the presence of  $-\text{NH}_2$  substituent as electron donor, whereas  $-\text{COOH}$  group conduces more negative charges of nitrogen imidazoles as electron acceptor. Meanwhile, the adsorption sites in other derivatives, such as  $-\text{CH}_3$  substituent and electron acceptor substituents like  $-\text{NO}_2$ ,  $-\text{COH}$ ,  $-\text{COOH}$ , lie in imidazole rings and oxygen, respectively. Therefore, more heteroatoms with negative partial atomic charges can create more adsorption sites.

**Table 4.** Mulliken charge of 4,5-diphenylimidazole derivatives by B3LYP/6-31G(d,p) CPCM(water) by the presence of electron-acceptor and donor substituents

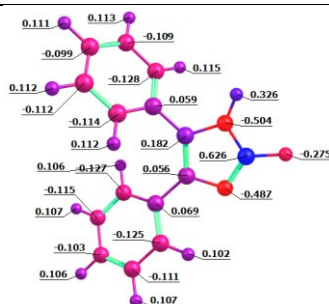
Inhibitor	Mulliken charge	Inhibitor	Mulliken charge
-----------	-----------------	-----------	-----------------







D-F



Furthermore, the inhibition efficiency of 4,5-diphenylimidazole conducted by DFT calculations (B3LYP 6-31G (d,p)) was determined by Equation 13-15 as follows (Obayes et al., 2014).

$$I_{\text{der}} \% = \frac{I_{\text{inh}} - I_{\text{X-inh}}}{I_{\text{inh}}} \times 100\% \quad [13]$$

$$IE_{\text{der}} \% = I_{\text{der}} \% \times IE_{\text{experiment}} \% \quad [14]$$

$$IE_{\text{theory}} \% = IE_{\text{der}} \% + IE_{\text{experiment}} \% \quad [15]$$

Annotation :

$I_{\text{der}} \%$  : Percentage of ionization potential 4,5-diphenylimidazole derivatives

$I_{\text{inh}}$  : Ionization potential of 4,5-diphenylimidazole compound

$I_{\text{X-inh}}$  : Ionization potential of 4,5-diphenylimidazole derivatives

$IE_{\text{der}} \%$  : Percentage of corrosion inhibition efficiency 4,5-diphenylimidazole derivatives

$IE_{\text{experiment}} \%$  : Percentage of experimentally corrosion inhibition efficiency 4,5-diphenylimidazole compound

$IE_{\text{theory}} \%$  : Theoretically corrosion inhibition efficiency of 4,5-diphenylimidazole derivatives

Tables 9 and 10 reveal inhibition efficiency theoretically depending on the ionization potential. 4,5-diphenylimidazole derivatives with  $-\text{NO}_2$ ,  $-\text{COH}$ , and  $-\text{COOH}$  substituents have relatively lower inhibition efficiency. On the other hand, 4,5-diphenylimidazole derivatives with electron-donor substituents show higher inhibition efficiency than other derivatives with electron-acceptor substituents. It corresponds to the higher ionization potential value and the lower number of electron transfers ( $\Delta N$ ). D- $\text{CH}_3$  is a better protector than D- $\text{CH}_2\text{CH}_3$ . Mulliken charge shifts of nitrogen elements affect those conditions, indicating the change in the reactivity of the inhibitor. D- $\text{NH}_2$  has the highest corrosion inhibition efficiency. D- $\text{NH}_2$  belongs to an influential adsorption center that protects the Fe surface. Therefore, this derivate theoretically performs better as a corrosion inhibitor than other derivatives.

**Table 5.** The theoretical inhibition efficiency of 4,5-diphenyl imidazole with electron acceptor and donor substituents in the aqueous phase

Corrosion Inhibitor	I/eV	I <sub>der</sub> /%	IE <sub>der</sub> /%	IE <sub>experiment</sub> /%	IE <sub>theory</sub> /%
4,5-diphenyl imidazole (D)	5.426			27.65	
D-NO <sub>2</sub>	5.935	-9.385	-2.595		25.055
D-Cl	5.518	-1.699	-0.470		27.180
D-COH	5.729	-5.590	-1.546		26.104
D-COOH	5.722	-5.470	-1.513		26.137
D-F	5.443	-0.326	-0.090		27.560
D-NH <sub>2</sub>	4.711	13.173	3.642		<b>31.292</b>
D-CH <sub>2</sub> OH	5.337	1.633	0.452		28.102
D-OH	5.135	5.358	1.481		29.131
D-CH <sub>3</sub>	5.281	2.674	0.739		28.389
D-CH <sub>2</sub> CH <sub>3</sub>	5.291	2.475	0.684		28.334

### Molecular Dynamics Simulation of Corrosion Inhibitor

Molecular dynamics simulation is useful for investigating interactions involving metal surfaces and inhibitors. This simulation was conducted to observe the interaction image as well as to predict the binding energy of 4,5-diphenyl imidazole and two types of its derivatives (D-NH<sub>2</sub> and D-NO<sub>2</sub>) with Fe. The equilibrium interactions of 4,5-diphenyl imidazole, D-NH<sub>2</sub>, and D-NO<sub>2</sub> with Fe(100) metal are depicted in Figure 5. Those inhibitor compounds have parallel configurations to the Fe(100) surface in the equilibrium condition. It can be related to the relatively uniform distribution of their HOMO and LUMO throughout the molecular structure (Leng et al., 2023). Besides that, this simulation also analyzes the adsorption behavior of studied molecules on the iron surface based on adsorption energy ( $E_{ads}$ ) in kcal.mol<sup>-1</sup> which is shown in Equation 16.

$$E_{ads} = E_{total} - (E_{Fe} - E_{inhibitor}) \quad [16]$$

$E_{total}$  is the total energy of complex Fe-inhibitor (kcal.mol<sup>-1</sup>),  $E_{Fe}$  is the energy of natural Fe (kcal.mol<sup>-1</sup>), and  $E_{inhibitor}$  is the energy of isolated inhibitor molecules (kcal.mol<sup>-1</sup>). Meanwhile, binding energy ( $E_{binding}$ ) was obtained from negative  $E_{ads}$ , or  $E_{binding} = -E_{ads}$ . The calculated binding energies are listed in Table 6. The results show that the binding energies from interactions between inhibitors and Fe surface are appreciable. It is in accordance with experimental inhibition efficiency (for 4,5-diphenyl imidazole), and theoretical inhibition efficiency is relatively low. Thus, the interaction with Fe metal on the surface tends to be unstable. The order of binding energy from these calculations is D-NH<sub>2</sub> > 4,5-diphenyl imidazole (D) > D-NO<sub>2</sub>.

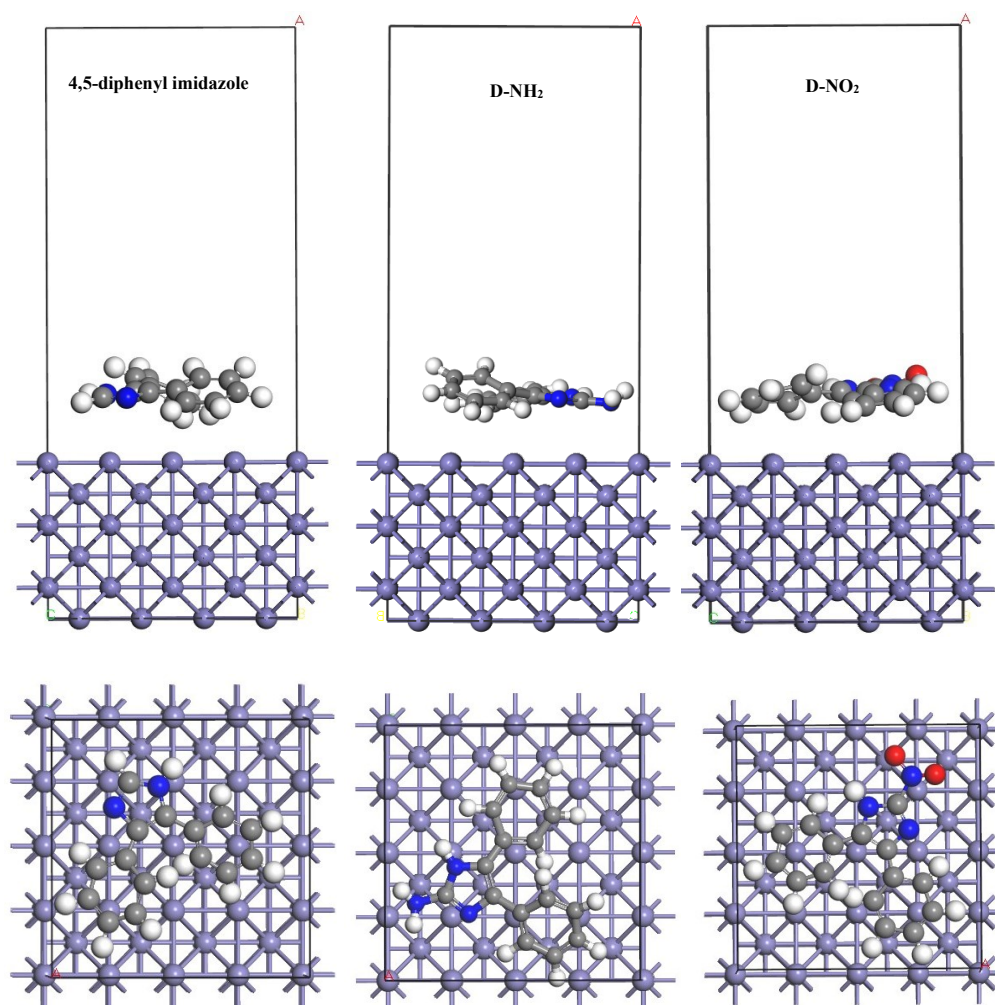


**Figure 5.** Adsorption configurations of 4,5-diphenyl imidazole, D-NH<sub>2</sub>, and D-NO<sub>2</sub> on the Fe(100) surface.

**Table 6.** Complex/total, adsorption, and binding energies (kcal.mol<sup>-1</sup>) of the three corrosion inhibitor molecules on the Fe(100) plane.

Corrosion Inhibitor	$E_{total}$	$E_{Fe}$	$E_{inh}$	$E_{ads}$	$E_{binding}$
4,5-diphenyl imidazole (D)	-9774.155	-9958.6711	245.7935	-61.2774	61.2774
D-NH <sub>2</sub>	-9881.104	-9958.6711	145.1912	-67.6241	67.6241
D-NO <sub>2</sub>	-9768.685	-9958.6711	228.5431	-38.5570	38.5570

## CONCLUSIONS

Corrosion inhibition performances of 4,5-diphenyl imidazole and its derivatives with additional electron withdrawing and electron donor substituents were computationally studied by quantum chemical calculations. The chemical quantum parameters obtained from the calculations can determine the inhibition performance of 4,5-diphenyl imidazole derivatives. A suitable corrosion inhibitor is indicated by high HOMO energy, chemical

softness, nucleophilicity, several electron transfers, back-donation energy, and interaction energy. In addition, low ionization energy, band gap energy, electronegativity, chemical hardness, and electrophilicity are other parameters of inhibitor performance. Meanwhile, LUMO energy and electron affinity parameters correspond to the ability of 4,5-diphenyl imidazole derivatives as mixed-type inhibitors. Theoretically, the 4,5-diphenylimidazole derivatives with  $-\text{NH}_2$  substituent showed higher corrosion inhibition efficiency ( $IE$ ) than other substituents depending on ionization potential. Thus, it will easily interact with the Fe atoms/ions to make protection. It can also improve the reactivity of the imidazole ring. Extra nitrogen in the  $-\text{NH}_2$  substituent and the oxygen atom in  $-\text{OH}$  and  $-\text{CH}_2\text{OH}$  substituents create additional adsorption centres in 4,5-diphenylimidazole derivatives based on Mulliken charges. Therefore, inserting  $\text{NH}_2$  substituent on 4,5-diphenylimidazole is helpful for better corrosion inhibition performance. Results of molecular dynamics simulation supported it.  $\text{D}-\text{NH}_2$  has higher binding energy than other derivatives. However, based on chemical softness, hardness, number of electron transfers, and back donation energy, a derivative with  $-\text{NO}_2$  substituent is a better inhibitor.

#### ACKNOWLEDGMENTS

The Authors would like to thank Universitas Sembilanbelas November Kolaka for funding this research to completion based on the Basic Research Scheme in 2023.

#### REFERENCES

- Al-Qurashi, O. S., & Wazzan, N. (2022). Molecular and periodic DFT calculations of the corrosion protection of Fe(1 1 0) by individual components of Aerva lanata flower as a green corrosion inhibitor. *Journal of Saudi Chemical Society*, 26(6), 101566. <https://doi.org/10.1016/j.jscs.2022.101566>.
- Allouche, A.-R. (2011). Gabedit—A graphical user interface for computational chemistry softwares. *Journal of Computational Chemistry*, 32(1), 174–182. <https://doi.org/https://doi.org/10.1002/jcc.21600>.
- Andersen, H. C. (1980). Molecular dynamics simulations at constant pressure and/or temperature. *The Journal of Chemical Physics*, 72(4), 2384–2393. <https://doi.org/10.1063/1.439486>
- Ashassi-Sorkhabi, H., Shaabani, B., & Seifzadeh, D. (2005). Effect of some pyrimidinic Schiff bases on the corrosion of mild steel in hydrochloric acid solution. *Electrochimica Acta*, 50(16–17), 3446–3452. <https://doi.org/10.1016/j.electacta.2004.12.019>.
- Baari, M. J. (2023). The oligosuccinimide and modified polysuccinimide as green corrosion and scale inhibitors. *Chimica Techno Acta*, 10(1), 1–19. <https://doi.org/10.15826/chimtech.2023.10.1.12>.
- Baari, M. J., Bundjali, B., & Wahyuningrum, D. (2021). Performance of *N,O*-Carboxymethyl Chitosan as Corrosion and Scale Inhibitors in  $\text{CO}_2$  Saturated Brine Solution. *Indonesian Journal of Chemistry*, 21(4), 954. <https://doi.org/10.22146/ijc.64255>.

- Baari, M. J., & Sabandar, C. W. (2021). A Review on Expired Drug-Based Corrosion Inhibitors: Chemical Composition, Structural Effects, Inhibition Mechanism, Current Challenges, and Future Prospects. *Indonesian Journal of Chemistry*, 21(5), 1316. <https://doi.org/10.22146/ijc.64048>.
- Bendjeddou, A., Abbaz, T., Gouasmia, A., & Villemin, D. (2016). Molecular Structure, HOMO-LUMO, MEP and Fukui Function Analysis of Some TTF-donor Substituted Molecules Using DFT (B3LYP) Calculations. *International Research Journal of Pure and Applied Chemistry*, 12(1), 1–9. <https://doi.org/10.9734/IRJPAC/2016/27066>.
- Chaussemier, M., Pourmohtasham, E., Gelus, D., Pécou, N., Perrot, H., Lédion, J., Horner, O. (2015). State of art of natural inhibitors of calcium carbonate scaling. A review article. *Desalination*, 356, 47–55. <https://doi.org/10.1016/j.desal.2014.10.014>.
- Chen, Z., Nong, Y., Chen, Y., Chen, J., & Yu, B. (2020). Study on the adsorption of OH<sup>-</sup> and CaOH<sup>+</sup> on Fe (100) surface and their effect on passivation of steel bar: Experiments and DFT modeling. *Corrosion Science*, 174, 108804. <https://doi.org/https://doi.org/10.1016/j.corsci.2020.108804>
- Elyoussfi, A., Daoudi, W., Salhi, A., Azghay, I., Ahari, M., Amhamdi, H., El Aatiaoui, A. (2023). Study of the effect nitro and hydroxyl substituents of two imidazopyridines derivatives on inhibitory efficacy: combining theoretical and experimental study (part A). *Journal of Applied Electrochemistry*, 53(11), 2169–2184. <https://doi.org/10.1007/s10800-023-01917-9>.
- Ghanbari, A., Attar, M. M., & Mahdavian, M. (2010). Corrosion inhibition performance of three imidazole derivatives on mild steel in 1M phosphoric acid. *Materials Chemistry and Physics*, 124(2–3), 1205–1209. <https://doi.org/10.1016/j.matchemphys.2010.08.058>.
- Guo, L., Ren, X., Zhou, Y., Xu, S., Gong, Y., & Zhang, S. (2017). Theoretical evaluation of the corrosion inhibition performance of 1,3-thiazole and its amino derivatives. *Arabian Journal of Chemistry*, 10(1), 121–130. <https://doi.org/10.1016/j.arabjc.2015.01.005>.
- Hanwell, M. D., Curtis, D. E., Lonie, D. C., Vandermeersch, T., Zurek, E., & Hutchison, G. R. (2012). Avogadro: an advanced semantic chemical editor, visualization, and analysis platform. *Journal of Cheminformatics*, 4(1), 17. <https://doi.org/10.1186/1758-2946-4-17>.
- Ismail, A., Irshad, H. M., Zeino, A., & Toor, I. H. (2019). Electrochemical Corrosion Performance of Aromatic Functionalized Imidazole Inhibitor Under Hydrodynamic Conditions on API X65 Carbon Steel in 1 M HCl Solution. *Arabian Journal for Science and Engineering*, 44(6), 5877–5888. <https://doi.org/10.1007/s13369-019->

03745-6.

- Kaya, S., Guo, L., Kaya, C., Tüzün, B., Obot, I. B., Touir, R., & Islam, N. (2016). Quantum chemical and molecular dynamic simulation studies for the prediction of inhibition efficiencies of some piperidine derivatives on the corrosion of iron. *Journal of the Taiwan Institute of Chemical Engineers*, 65, 522–529. <https://doi.org/10.1016/j.jtice.2016.05.034>.
- Knizia, G. (2013). Intrinsic Atomic Orbitals: An Unbiased Bridge between Quantum Theory and Chemical Concepts. *Journal of Chemical Theory and Computation*, 9(11), 4834–4843. <https://doi.org/10.1021/ct400687b>.
- Leng, M., Xue, Y., Luo, L., & Chen, X. (2023). Insight into the effect of functional groups on the inhibition performance for imidazoline: DFT and MD simulations. *Computational and Theoretical Chemistry*, 1229(July), 114327. <https://doi.org/10.1016/j.comptc.2023.114327>
- Lv, J., Fu, L., Zeng, B., Tang, M., & Li, J. (2019). Synthesis and Acidizing Corrosion Inhibition Performance of N-Doped Carbon Quantum Dots. *Russian Journal of Applied Chemistry*, 92(6), 848–856. <https://doi.org/10.1134/S1070427219060168>.
- Madkour, L. H., & Elroby, S. K. (2015). Inhibitive properties, thermodynamic, kinetics and quantum chemical calculations of polydentate Schiff base compounds as corrosion inhibitors for iron in acidic and alkaline media. *International Journal of Industrial Chemistry*, 6(3), 165–184. <https://doi.org/10.1007/s40090-015-0039-7>.
- Madkour, L. H., & Elshamy, I. H. (2016). Experimental and computational studies on the inhibition performances of benzimidazole and its derivatives for the corrosion of copper in nitric acid. *International Journal of Industrial Chemistry*, 7(2), 195–221. <https://doi.org/10.1007/s40090-015-0070-8>.
- Martinović, I., Pilić, Z., Zlatić, G., Barišić, M., & Čelan, S. (2021). Corrosion Inhibition of Aluminium by *Alchemilla vulgaris* L. Extract in 3 % NaCl Solution. *Croatica Chemica Acta*, 94(2), 103–109. <https://doi.org/10.5562/cca3858>.
- Marušić, K., Otmačić Čurković, H., Supnišek Lisac, E., & Takenouti, H. (2018). Two Imidazole Based Corrosion Inhibitors for Protection of Bronze from Urban Atmospheres. *Croatica Chemica Acta*, 91(4), 435–446. <https://doi.org/10.5562/cca3440>.
- Mi, H., Xiao, G., & Chen, X. (2015). Theoretical evaluation of corrosion inhibition performance of three antipyrine compounds. *Computational and Theoretical Chemistry*, 1072, 7–14. <https://doi.org/https://doi.org/10.1016/j.comptc.2015.08.023>
- Mustafa, D., & Mamand, D. (2019). *Theoretical Calculations and Spectroscopic Analysis of Gaussian Computational Examination-NMR, FTIR, UV-Visible, MEP on 2,4,6-Nitrophenol*.



- Neese, F. (2022). Software update: The <scp>ORCA</scp> program system—Version 5.0. *WIREs Computational Molecular Science*, 12(5), e1606. <https://doi.org/10.1002/wcms.1606>.
- Neese, F., Wennmohs, F., Ganyushin, D., Garcia, M., Guo, Y., Hansen, A., ... Huntington, L. (2022). *Orca 5.0.3*.
- Obayes, H. R., Alwan, G. H., Alobaidy, A. H. M. J., Al-Amiery, A. A., Kadhum, A. A. H., & Mohamad, A. B. (2014). Quantum chemical assessment of benzimidazole derivatives as corrosion inhibitors. *Chemistry Central Journal*, 8(1), 21. <https://doi.org/10.1186/1752-153X-8-21>.
- Obot, I. B., Kaya, S., Kaya, C., & Tüzün, B. (2016). Density Functional Theory (DFT) modeling and Monte Carlo simulation assessment of inhibition performance of some carbonyl Schiff bases for steel corrosion. *Physica E: Low-Dimensional Systems and Nanostructures*, 80, 82–90. <https://doi.org/10.1016/j.physe.2016.01.024>
- Ouakki, M., Galai, M., Rbaa, M., Abousalem, A. S., Lakhrissi, B., Rifi, E. H., & Cherkaoui, M. (2019). Quantum chemical and experimental evaluation of the inhibitory action of two imidazole derivatives on mild steel corrosion in sulphuric acid medium. *Heliyon*, 5(11), e02759. <https://doi.org/10.1016/j.heliyon.2019.e02759>.
- Oyeneyin, O. E., Ojo, N. D., Ipinloju, N., Agbaffa, E. B., & Emmanuel, A. V. (2022). Investigation of the corrosion inhibition potentials of some 2-(4-(substituted)arylidene)-1H-indene-1,3-dione derivatives: density functional theory and molecular dynamics simulation. *Beni-Suef University Journal of Basic and Applied Sciences*, 11(1), 132. <https://doi.org/10.1186/s43088-022-00313-0>.
- Qiang, Y., Zhang, S., Yan, S., Zou, X., & Chen, S. (2017). Three indazole derivatives as corrosion inhibitors of copper in a neutral chloride solution. *Corrosion Science*, 126, 295–304. <https://doi.org/10.1016/j.corsci.2017.07.012>.
- Quy Huong, D., Duong, T., & Nam, P. C. (2019). Effect of the Structure and Temperature on Corrosion Inhibition of Thiourea Derivatives in 1.0 M HCl Solution. *ACS Omega*, 4(11), 14478–14489. <https://doi.org/10.1021/acsomega.9b01599>.
- Revie, R. W., & Uhlig, H. H. (2008). Definition and Importance of Corrosion. In *Corrosion and Corrosion Control* (pp. 1–8). Hoboken, NJ, USA: John Wiley & Sons, Inc. <https://doi.org/10.1002/9780470277270.ch1>.
- Rodríguez-Valdez, L. M., Martínez-Villafañe, A., & Glossman-Mitnik, D. (2005). CHIH-DFT theoretical study of isomeric thiazoles and their potential activity as corrosion inhibitors. *Journal of Molecular Structure: THEOCHEM*, 716(1–3), 61–65. <https://doi.org/10.1016/j.theochem.2004.10.082>.
- Srivastava, V., Haque, J., Verma, C., Singh, P., Lgaz, H., Salghi, R., & Quraishi, M. A.

- (2017). Amino acid based imidazolium zwitterions as novel and green corrosion inhibitors for mild steel: Experimental, DFT and MD studies. *Journal of Molecular Liquids*, 244, 340–352. <https://doi.org/10.1016/j.molliq.2017.08.049>.
- Subekti, N., Soedarsono, J. W., Riastuti, R., & Sianipar, F. D. (2020). Development of environmental friendly corrosion inhibitor from the extract of areca flower for mild steel in acidic media. *Eastern-European Journal of Enterprise Technologies*, 2(6–104), 34–45. <https://doi.org/10.15587/1729-4061.2020.197875>.
- Tsuneda, T. (2014). *Density Functional Theory in Quantum Chemistry*. <https://doi.org/10.1007/978-4-431-54825-6>.
- Wahyuningrum, D. (2008). *Sintesis Senyawa Turunan Imidazol Dan Penentuan Aktivitas Inhibisi Korosinya Pada Permukaan Baja Karbon*. Disertasi. Bandung. Institut Teknologi bandung.
- Wang, D., Li, Y., Chen, B., & Zhang, L. (2020). Novel surfactants as green corrosion inhibitors for mild steel in 15% HCl: Experimental and theoretical studies. *Chemical Engineering Journal*, 402, 126219. <https://doi.org/10.1016/j.cej.2020.126219>.
- Wazzan, N. A. (2015). DFT calculations of thiosemicarbazide, arylisothiocyanates, and 1-aryl-2,5-dithiohydrazodicarbonamides as corrosion inhibitors of copper in an aqueous chloride solution. *Journal of Industrial and Engineering Chemistry*, 26, 291–308. <https://doi.org/10.1016/j.jiec.2014.11.043>.
- Wazzan, N. A., & Mahgoub, F. M. (2014). DFT Calculations for Corrosion Inhibition of Ferrous Alloys by Pyrazolopyrimidine Derivatives. *Open Journal of Physical Chemistry*, 04(01), 6–14. <https://doi.org/10.4236/ojpc.2014.41002>.
- Xiang, Y., Long, Z., Li, C., Huang, H., & He, X. (2017). Inhibition of N80 steel corrosion in impure supercritical CO<sub>2</sub> and CO<sub>2</sub>-saturated aqueous phases by using imino inhibitors. *International Journal of Greenhouse Gas Control*, 63, 141–149. <https://doi.org/10.1016/j.ijggc.2017.05.010>.
- Zarrouk, A., El Ouali, I., Bouachrine, M., Hammouti, B., Ramli, Y., Essassi, E. M., Salghi, R. (2013). Theoretical approach to the corrosion inhibition efficiency of some quinoxaline derivatives of steel in acid media using the DFT method. *Research on Chemical Intermediates*, 39(3), 1125–1133. <https://doi.org/10.1007/s11164-012-0671-1>.
- Zhurko, G. and Zhurko, D. (2015). Chemcraft Graphical Program for Visualization of Computed Results. Retrieved from <http://www.chemcraftprog.com/>
- Zunita, M., Wahyuningrum, D., Buchari, Bundjali, B., Wenten, I. G., & Boopathy, R. (2020). Corrosion Inhibition Performances of Imidazole Derivatives-Based New Ionic Liquids on Carbon Steel in Brackish Water. *Applied Sciences*, 10(20), 7069. <https://doi.org/10.3390/app10207069>.